HHS Public Access

Author manuscript

Neurobiol Dis. Author manuscript; available in PMC 2023 July 10.

Published in final edited form as:

Neurobiol Dis. 2023 May ; 180: 106099. doi:10.1016/j.nbd.2023.106099.

The serine hydrolase ABHD6 controls survival and thermally induced seizures in a mouse model of Dravet syndrome

Ruth Westenbroek[a], **Joshua Kaplan**[a,b], **Katie Viray**[a], **Nephi Stella**[a,c,*]

[a]Department of Pharmacology, University of Washington School of Medicine, Seattle, WA 98195, USA

[b]Department of Psychology, Western Washington University, Bellingham, WA 98225, USA

[c]Department of Psychiatry and Behavioral Sciences, University of Washington School of Medicine, Seattle, WA 98195, USA

Abstract

Evidence suggests that inhibition of α/β hydrolase-domain containing 6 (**ABHD6**) reduces seizures; however, the molecular mechanism of this therapeutic response remains unknown. We discovered that heterozygous expression of *Abhd6* (*Abhd6*$^{+/-}$) significantly reduced the premature lethality of *Scn1a*$^{+/-}$ mouse pups, a genetic mouse model of Dravet Syndrome (**DS**). Both *Abhd6*$^{+/-}$ mutation and pharmacological inhibition of ABHD6 reduced the duration and incidence of thermally induced seizures in *Scn1a*$^{+/-}$ pups. Mechanistically, the in vivo anti-seizure response resulting from ABHD6 inhibition is mediated by potentiation of gamma-aminobutyric acid receptors Type-A (**$GABA_AR$**). Brain slice electrophysiology showed that blocking ABHD6 potentiates extrasynaptic (tonic) $GABA_AR$ currents that reduce dentate granule cell excitatory output without affecting synaptic (phasic) $GABA_AR$ currents. Our results unravel an unexpected mechanistic link between ABHD6 activity and extrasynaptic $GABA_AR$ currents that controls hippocampal hyperexcitability in a genetic mouse model of DS.

Brief summary: This study provides the first evidence for a mechanistic link between ABHD6 activity and the control of extrasynaptic $GABA_AR$ currents that controls hippocampal hyperexcitability in a genetic mouse model of Dravet Syndrome and can be targeted to dampened seizures.

*Corresponding author at: HSC BB1504A, 1959 NE Pacific St, Seattle, WA 98195-7280, USA. nstella@uw.edu (N. Stella).

CRediT authorship contribution statement

Ruth Westenbroek: Conceptualization, Methodology, Funding acquisition, Writing – original draft, Writing – review & editing. **Joshua Kaplan:** Conceptualization, Methodology, Writing – original draft, Writing – review & editing. **Katie Viray:** Methodology, Project administration, Writing – review & editing. **Nephi Stella:** Conceptualization, Funding acquisition, Supervision, Writing – original draft, Writing – review & editing.

Appendix A. Supplementary data

Supplementary data to this article can be found online at https://doi.org/10.1016/j.nbd.2023.106099.

Declaration of Competing Interest

R.W., J.K. and K.V. reported no financial interests or potential conflicts of interest. N.S. is employed by Stella Consulting LLC. The terms of this arrangement have been reviewed and approved by the University of Washington in accordance with its policies governing outside work and financial conflicts of interest in research.

Keywords

Dravet syndrome; Seizures; Epilepsy; GABA receptors

1. Introduction

The recently discovered multifunction serine-hydrolase, ABHD6, regulates several facets of neurotransmission. For example, pharmacological inhibition of ABHD6 results in local increases of 2-arachidonoyl-glycerol (**2-AG**) levels, a signaling lipid that enhances the activity of multiple receptors, including $GABA_AR$, cannabinoid CB_1 receptors (**CB_1R**) and CB_2R (Cao et al., 2019). The therapeutic efficacy of first generation ABHD6 inhibitors has been reported in several preclinical mouse models of neurological diseases, including experimental autoimmune encephalomyelitis, traumatic brain injury and epilepsy (Manterola et al., 2018; Naydenov et al., 2014; Tchantchou and Zhang, 2013; Wen et al., 2015; Zareie et al., 2018). Relevant here, the first generation ABHD6 inhibitor, WWL70, reduces PTZ-induced seizures in wildtype mice, and this therapeutic response is unaffected in $CB_1R^{-/-}$ and $CB_2R^{-/-}$ mice treated with PTZ, indicating that activation of CB_1R and CB_2R is not involved in the anti-seizure response of ABHD6 inhibitors (Naydenov et al., 2014). The involvement of $GABA_AR$ in mediating the anti-seizure response of ABHD6 inhibition was suggested by pretreating mice with a subconvulsive dose of picrotoxin (**PTX**, 1 mg/kg) that does not affect PTZ-triggered seizures per se and yet prevents the anti-seizure response of WWL70 (Naydenov et al., 2014). Significantly, genetic deletion of ABHD6 and semi-chronic treatment with first generation ABHD6 inhibitors is not associated with side-effects and has little effect in healthy behaving mice, suggesting that these agents have a promising safety profile (Deng et al., 2021). Furthermore, semi-chronic inhibition of ABHD6 is not associated with tolerance, an important quality for potential new therapeutic modalities (Deng et al., 2021; Naydenov et al., 2014). Thus, ABHD6 inhibitors are emerging as promising therapeutic agents for the treatment of seizures, but their efficacy and mechanism in preclinical mouse models of intractable childhood epilepsy disorders has not been tested, nor has the precise molecular and cellular mechanism of this therapeutic response been uncovered.

DS is an intractable childhood epilepsy disorder characterized by a high rate of premature death and severe co-morbidities, including spontaneous and thermal sensitive seizures, developmental delays and cognitive impairments (Dravet, 2011). This syndrome is primarily caused by dominant, heterozygous loss-of-function mutations in the gene *SCN1A* encoding the brain sodium channel Nav1.1 (Catterall, 2017). Mechanistically, *Scn1a* mutations reduce sodium currents primarly in GABAergic interneurons, which impairs their electrical excitability, creates an imbalance in the ratio of excitation and inhibition in neural circuits, and promotes general hyperexcitability and seizures (Colasante et al., 2020; Kalume et al., 2013; Liautard et al., 2013; Martin et al., 2010; Ogiwara et al., 2007; Yu et al., 2006). Multiple genetic mouse models of DS have been developed that recapitulate key pathological features and clinical phenotypes known in patients diagnosed with DS and have been preclinically validated (Griffin et al., 2018). Such models serve as precision medicine tools for testing treatments of epileptic syndroms caused by single genetic mutations.

Current anti-seizure medicines (**AEM**) generally do not fully control seizures in patients diagnosed with DS and their use is often associated with severe side-effects, emphasizing the need to develop new therapeutic approaches that act through different mechanisms of action. Here we tested if ABHD6 blockade reduces lethality and seizures in the *Scn1a*$^{+/-}$ mouse model of DS, and studied the molecular mechanism of this therapeutic response by electrophysiological assessments of hippocampal slices.

2. Results

2.1. Heterozygous deletion of Abhd6 rescues premature death in Scn1a$^{+/-}$ mice

$Na_V1.1$ channels encoded by *Scn1a* play an essential role in the generation of action potentials (**AP**), repetitive neuronal firing and development. Accordingly, homozygous loss of function mutations, *Scn1a*$^{-/-}$, are embryonically lethal and only a small fraction of *Scn1*$^{+/-}$ pups survive until PND21 (weaning) (Yu et al., 2006). Furthermore, the disease progression in the *Scn1a*$^{+/-}$ mice changes in nature with age; it begins with reduced viability of *Scn1a*$^{+/-}$ pups that is independent of seizures and occurs between PND0 and before weaning (PND1–21), which is then followed by a period of increased seizure susceptibility and risk of SUDEP (PND21–35) (Kalume et al., 2013). Mice that survive this critical period eventually exhibit pronounced behavioral impairments (Ito et al., 2013). Little is known about the molecular changes that occur in mice that survive the increased seizure susceptibility period (PND35–90).

To determine if genetic deletion of *Abhd6* influences the survival of *Scn1*$^{+/-}$ pups, we crossed *Scn1a*$^{+/-}$ mice with *Abhd6*$^{-/-}$ mice to generate *Scn1a*$^{+/-}$; *Abhd6*$^{+/-}$ pups and *Scn1a*$^{+/-}$; *Abhd6*$^{-/-}$ pups (Fig. 1A). Of note, the *Scn1a* and *Abhd6* genes are on different chromosomes (2 and 6, respectively) and thus follow Mendelian distribution. We first monitored the number of litters that survived until weaning (i. e., litters of at least 1 pup at PND21), an index of seizure-independent lethality occurring in *Scn1*$^{+/-}$ progenies. Fig. 1B shows that, as expected, 100% of the litters delivered by WT X WT breeders, WT X *Abhd6*$^{-/-}$ breeders and *Abhd6*$^{+/-}$ X *Abhd6*$^{+/-}$ breeders survived until PND21 (Deng et al., 2021), whereas only 63% of the litters delivered by WT X *Scn1a*$^{+/-}$ breeders survived until PND21 (Yu et al., 2006). Fig. 1B also shows that 50% of litters delivered by *Scn1a*$^{+/-}$ X *Abhd6*$^{+/-}$ breeders and 54% of litters delivered by *Scn1a*$^{+/-}$ X *Abhd6*$^{-/-}$ breeders survived until PND21. Furthermore, the *Abhd6*$^{+/-}$ and *Abhd6*$^{-/-}$ mutations did not influence the average number of pups per litters (Fig. 1C). These results show that introducing *Abhd6*$^{+/-}$ and *Abhd6*$^{-/-}$ mutations in the *Scn1a*$^{+/-}$ mouse line does not influence the mortality rate associated with *Scn1a*$^{+/-}$ before PND21.

We then monitored survival starting at PND21 and found that *Abhd6*$^{+/-}$ rescued the premature lethality of *Scn1a*$^{+/-}$ pups, whereas *Abhd6*$^{-/-}$ accelerated the premature lethality of *Scn1a*$^{+/-}$ pups (Fig. 1D). Thus, a clear increase in survival was observed after PND25, which resulted in 80% of *Scn1a*$^{+/-}$; *Abhd6*$^{+/-}$ pups surviving until PND90 as compared to 41% of the *Scn1a*$^{+/-}$ pups surviving until PND90. By contrast, *Scn1a*$^{+/-}$; *Abhd6*$^{-/-}$ pups succumbed at a much faster rate than *Scn1a*$^{+/-}$ pups and did not survive beyond PND48. These results show that *Abhd6*$^{+/-}$ reduces *Scn1a*$^{+/-}$ mice lethality during the period of increased seizure susceptibility, whereas *Abhd6*$^{-/-}$ accelerates it.

2.2. Heterozygous deletion and pharmacological inhibition of ABHD6 reduce thermally induced seizures in Scn1a$^{+/-}$ mice in a GABA$_A$R-dependent manner

Based on the results of Fig. 1, we hypothesized that ABHD6 might represent a tractable enzyme to modulate in order to reduce seizures in *Scn1a*$^{+/-}$ mice. Accordingly, we tested whether *Abhd6*$^{+/-}$ and *Abhd6*$^{-/-}$ genotypes differentially influence thermally induced seizures in *Scn1a*$^{+/-}$ pups. Febrile seizures are often the first symptom of DS, arising at 6–9 months of age in humans, and they are reliably modelled by thermal induction of seizures in *Scn1a*$^{+/-}$ pups shortly after PND 21 (Catterall, 2017; Dravet, 2011). To measure the susceptibility of *Scn1a*$^{+/-}$ pups (PND21–35) to thermal seizures, their body temperature was increased by 0.5 °C every 2 min until either a seizure occurred, or the body temperature reached 41 °C (Fig. 2A-B). As soon as a behavioral seizure was detected, the heating source was turned off, and the behavioral seizure was evaluated by review of video recordings. As previously shown, WT mice did not experience behavioral seizures when elevating body temperature to 41 °C (i.e., 100% of mice remained seizure free), whereas half of *Scn1a*$^{+/-}$ mice exhibited behavioral seizures at 38.4 ± 0.2 °C (i. e., 50% of *Scn1a*$^{+/-}$ mice experienced seizures at that temperature or lower, Supplementary Fig. S1A) (Yu et al., 2006). Signficantly, while the average temperature reached to induce seizures remained at 38.4 ± 0.3 °C in *Scn1a*$^{+/-}$; *Abhd6*$^{+/-}$ pups, the duration of thermally induced seizures was significantly reduced in *Scn1a*$^{+/-}$; *Abhd6*$^{+/-}$ pups (32 ± 5 s) compared to *Scn1a*$^{+/-}$ pups (52 ± 6 s) (Fig. 2C-D). Both *Scn1a*$^{+/-}$ and *Scn1a*$^{+/-}$; *Abhd6*$^{+/-}$ pups exhibited generalized tonic-clonic seizures, rearing, clonus, and/or falling over seizures (i.e., Racine scale 5) (Supplementary Fig. S1B).

To determine whether pharmacological inhibition of ABHD6 also controls thermal seizures in *Scn1a*$^{+/-}$ mice, we tested KT-182, a second generation ABHD6 inhibitor, at 2 mg/kg, i.p., at dose shown to rapidly inhibit brain ABHD6 activity (Hsu et al., 2013). KT-182 (2 mg/kg, i.p.) also reduced the duration of thermal seizure of *Scn1a*$^{+/-}$ mice to 36 ± 4 s without affecting the average temperature of thermally induced seizures or seizure severity (Figs. 2C-D and Supplementary Fig. S1B). KT-182 similarly reduced seizure duration in *Scn1a*$^{+/-}$ pups PND24–27 and PND29–35 despite the known age-dependent increase in seizure duration (Supplementary Fig. S2). In our previous study, we showed that treatment of mice with a subthreshold dose of the GABA$_A$R antagonist PTX (1 mg/kg, i.p.), which does not affect PTZ-triggered seizures in wildtype mice per se, nevertheless fully prevents the anti-seizure response of ABHD6 inhibition, suggesting that ABHD6 inhibition results in a potentiation of GABA$_A$R function (Naydenov et al., 2014). Here we use a similar approach to test whether GABA$_A$R are also involved in the anti-seizure response of ABHD6 inhibition in *Scn1a*$^{+/-}$ mice (PND21–35). Fig. 2D shows that pretreating *Scn1a*$^{+/-}$ pups with the same regimen of PTX (i.e., 1 mg/kg, i.p. that does not affect thermally induced seizures per se) fully prevented the anti-seizure response of both *Abhd6*$^{+/-}$ mutation and ABHD6 pharmacological inhibition with KT-182. Subthreshold treatment with PTX did not influence the average temperature of thermally induced seizures and seizure severities (Fig. 2C and Supplementary Fig. S1B). These results show that the reduction in the duration of thermally induced seizures in *Scn1a*$^{+/-}$ pups also involves a potentiation of GABA$_A$Rs function.

Patients diagnosed with DS suffer from seizures when their body temperature rises due to hot baths and fevers (Korff et al., 2007; Xu et al., 2014). We evaluated the potential therapeutic value of ABHD6 pharmacologocial inhibition against seizures triggered by a rise in body temperature that mimics low-grade fevers (38 °C) in *Scn1a*$^{+/-}$ pups. We found a greater percent of KT-182-treated *Scn1a*$^{+/-}$ pups that were seizure-free compared to *Scn1a*$^{+/-}$ pups (11.1% and 21.4%, respectively, $n = 7$ and 11 pups, respectively). For those that exhibited seizures, KT-182-treated pups exhibited shorter seizures (from 51 ± 11 to 28 ± 2 s, respectively), and no change in seizure frequency (vehicle treatment = 2.6 seizures/animal, and KT-182 treatment = 3.2 seizures/animal) or in seizure severity (Supplementary fig. S2). These results indicate that ABHD6 inhibition tested in an experimental paradigm that mimics low-to-moderate fever both increases the likelihood of being seizure free and reduces the duration of seizures that occur. Thus, ABHD6 inhibition shows anti-seizure therapeutic value in a preclinical model of DS when using physiological triggers of seizures.

2.3. Homozygous deletion of ABHD6 reduces thermally induced seizures in Scn1a$^{+/-}$ mice

Reduced survival of *Scn1a*$^{+/-}$; *Abhd6*$^{-/-}$ mice compared to *Scn1a*$^{+/-}$ mice suggests that complete loss of ABHD6 expression might enhance and accelerate *Scn1a*$^{+/-}$ mice pathogenesis shortly after PND21. One possibility is that *Scn1a*$^{+/-}$; *Abhd6*$^{-/-}$ pups exhibit exacerbated seizures. Despite the low survival yield of *Scn1a*$^{+/-}$; *Abhd6*$^{-/-}$ pups, we were able to study the thermal-induced behavioral seizure in seven individuals, and found that the duration of their thermally induced seizures were reduced to the same extent as *Abhd6*$^{+/-}$ mutation and KT-182 treatment, and that seizure severity and temperature of induction remained comparable to *Scn1a*$^{+/-}$ pups (Fig. 2C-D). PTX treatment of *Scn1a*$^{+/-}$; *Abhd6*$^{-/-}$ pups also prevented the anti-seizure response but also reduced the temperature required to trigger seizures (Fig. 2C-D). Together, these results show that both *Abhd6*$^{+/-}$ and *Abhd6*$^{-/-}$ rescue thermally induced seizures in *Scn1a*$^{+/-}$ mice to the same extent and suggest that *Abhd6*$^{-/-}$ mutations might accelerate *Scn1a*$^{+/-}$ lethality through a seizure-independent mechanism.

2.4. ABHD6 inhibition reduces the excitation of hippocampal granule cells in the dentate gyrus

To better understand the molecular mechanism that mediates the anti-seizure effects of ABHD6 inhibition, we studied its effect on hippocampal granule cells (**GCs**) in the dentate gyrus (**DG**) using slice electrophysiology. Overexcitation of these cells causes seizures in epileptic patients and rodent models (Dengler and Coulter, 2016; Krook-Magnuson et al., 2015); therefore, pharmacological strategies that dampen excitatory transmission projecting from the DG could protect against seizure onset and impede seizure propagation. We performed current-clamp recordings of GCs in hippocampal slices from *Scn1a*$^{+/-}$ pups and tested the effect of KT-182 on action potential (**AP**) frequency (Fig. 3A). We started by studying hippocampal slices from *Scn1a*$^{+/-}$ pups at PND35–45 (i.e., individuals that survived the early critical period of enhanced spontaneous seizures and SUDEP). Figs. 3B-C show that KT-182 (100 nM) reduced the AP frequency of GCs and that this response was absent when slices were pretreated with the broad spectrum $GABA_AR$ antagonist, GABAzine, that increased AP frequency. These results suggests that ABHD6 inhibition

reduces excitatory output from the DG through a $GABA_AR$-mediated mechanism. Values and statistically significant outcomes of electrophysiology recordings are in Supplementary Table S1.

To further decipher this response, we tested the effect of ABHD6 inhibition on both inhibitory and excitatory postsynaptic currents (sIPSCs and sEPSCs) by performing whole-cell voltage-clamp recordings of GCs in *Scn1a*$^{+/-}$ hippocampal slices (PND35–45). Fig. 3D and F show that the frequency of sIPSCs was not affected by KT-182 (100 nM), indicating that ABHD6 inhibition increases post-synaptic $GABA_AR$ currents without affecting the frequency of synaptic (phasic) GABA release. Significantly, sEPSC frequency was decreased by KT-182 (−33.4 ± 11.1%, $n = 6$) and this response was absent in GABAzine pretreated slices, supporting the involvement of post-synaptic $GABA_AR$ that control excitatory transmission (Fig. 3E-F). Together, these results show that ABHD6 inhibition reduced the excitability of GC through a mechanism that is independent of postsynaptic (phasic) $GABA_ARs$ mediated sIPSCs, suggesting the involvement of extrasynaptic (tonic) $GABA_ARs$.

2.5. ABHD6 inhibition enhances tonic $GABA_AR$-mediated inhibition in granule cells

To test if ABHD6 inhibition influences tonic $GABA_AR$-mediated currents in GCs of *Scn1a*$^{+/-}$ hippocampal slices (PND35–45), we performed whole-cell recordings in the voltage-clamp configuration ($E_{Cl-} = 0$ mV and $V_h = -60$ mV). Figs. 4A-B show that tonic $GABA_AR$-mediated currents in GCs of *Scn1a*$^{+/-}$ hippocampal slices were similarly enhanced by 100 nM and 1 mM KT-182. This KT-182 response was blocked by GABAzine, suggesting that it was caused by potentiation of extrasynaptic (tonic) $GABA_AR$ currents (Fig. 4C-D). Fig. 4E shows that the KT-182-potentiation of tonic $GABA_AR$-mediated currents in GCs of *Scn1a*$^{+/-}$ hippocampal slices was unaffected by adding GABA (200 nM), confirming that our slice conditions were sufficient for detecting KT-182 s effects on tonic current amplitudes and does not depend endogenous GABA. Significantly, the KT-182-potentiation of tonic $GABA_AR$-mediated currents in GCs was greater in *Scn1a*$^{+/-}$ hippocampal slices (PND35–45) compared to WT slices, and was absent in *Abhd6*$^{-/-}$ (Fig. 4E). Together, these results show that ABHD6 inhibition potentiates extrasynaptic (tonic) $GABA_AR$ currents in *Scn1a*$^{+/-}$ hippocampal slices from PND35–45 mice (Fig. 4D). These results also suggest that ABHD6 inhibition in *Scn1a*$^{+/-}$ mice may lead to more pronounced effects on tonic inhibition as compared to WT mice, perhaps due to greater capacity to mediate a tonic current.

To address this possibility, we measured the capacity of THIP, an agonist of the δ subunit of extrasynaptic $GABA_ARs$ (Meera et al., 2011), to trigger tonic inhibition in GCs from WT and *Scn1a*$^{+/-}$ hippocampal slices at P20 and P35–45 (i.e., before and after the increased seizure susceptibility, respectively). Fig. 5A, B shows that before the critical period, the amplitude of the THIP-induced tonic inhibitory current in dentate GCs was similar in WT and *Scn1a*$^{+/-}$ slices, and this response approximately doubled in dentate GCs from *Scn1a*$^{+/-}$ compared to WT after the critical period (Fig. 5C, D). This result suggests that there is a compensatory mechanism that is activated during the period of elevated seizure susceptibility (P21-P35), which leads to an enhanced capacity for tonic inhibition through

extrasynaptic $GABA_AR$ in *Scn1a*$^{+/-}$ pups. Significantly, since ABHD6 inhibition enhances tonic inhibitory currents mediated by extrasynaptic $GABA_AR$ in GCs, these results also suggest that the therapeutic efficacy of ABHD6 inhibitors may be bolstered by enhanced extrasynaptic $GABA_AR$ function in surviving *Scn1a*$^{+/-}$ pups.

3. Discussion

We discovered a novel molecular interaction that links ABHD6 activity to extrasynaptic (tonic) $GABA_AR$ currents in GCs and controls hippocampal excitatory output in a preclinical mouse model of DS. It is well-known that activation of extrasynaptic d-subunit-containing $GABA_AR$ increases tonic inhibitory currents and controls neuronal excitability differently than phasic activation of synaptic $GABA_AR$, which do not contain d-subunits (Brickley and Mody, 2012). Tonic $GABA_AR$ currents generate long-lasting inhibition that controls network excitability and hippocampal rhythmogenesis, a shunting inhibition mechanism that decreases AP frequency and neuronal hyperexcitability (Schipper et al., 2016). We also show that both pharmacological inhibition of ABHD6 and heterozygote *Abhd6* mutation in *Scn1a*$^{+/-}$ pups reduce the incidence and duration of thermally induced seizures during the critical period associated with increase seizure susceptibility and mortality. Signficantly, tonic $GABA_AR$ currents in GCs of surviving *Scn1a*$^{+/-}$ pups are increased, a compensatory mechanism that might contribute to the therapeutic efficacy of ABHD6 inhibition. Together, our results suggest a molecular mechanism whereby inhibiting ABHD6 activity in *Scn1a*$^{+/-}$ hippocampal GCs potentiates tonic $GABA_AR$ inhibitory currents, reduces hippocampal hyperexcitatory output, and lowers seizure incidence and duration.

3.1. A novel molecular interaction

What is the likely molecular link between ABHD6 inhibition and potentiation of tonic $GABA_AR$ currents? Several mechanisms are known to increase tonic $GABA_AR$ currents, including repetitive depolarization of GABAergic neurons that enhances extrasynaptic GABA diffusion and triggers non-vesicular GABA release (McCartney et al., 2007; Schipper et al., 2016; Wlodarczyk et al., 2013), as well as an increase in the production of endogenous positive allosteric modulators, such as neurosteroids and the signaling lipid 2-AG (Rudolph and Knoflach, 2011). Considering that ABHD6 both hydrolyzes 2-AG and is expressed in postsynaptic terminals, 2-AG represents the most likely candidate that links ABHD6 inhibition to potentiation of $GABA_AR$ currents. Specifically, 2-AG binds to an intracellular allosteric binding site on $GABA_AR$, suggesting that localized subcellular increases in post-synaptic 2-AG due to ABHD6 inhibition are likely sufficient to potentiate tonic $GABA_AR$ currents (Bakas et al., 2017; Sigel et al., 2011).

Furthermore, 2-AG (0.3–30 mM) allosterically increase $GABA_AR$ currents by 4-fold though a mechanism that does not involve the benzodiazepine (**BDZ**) and neurosteroid binding sites (Anderson et al., 2019; Golovko et al., 2014). Note that, compared to synaptic $GABA_ARs$, extrasynaptic $GABA_ARs$ exhibit increased sensitivity to neurosteroids and low sensitivity to BDZ, underscoring the novety of this molecular interaction between ABHD6 and extrasynaptic $GABA_ARs$ (Chuang and Reddy, 2018).

3.2. Abhd6 mutations and Scn1a+/− survival

The disease progression that develops in *Scn1a*$^{+/-}$ mice results in changing phenotypes from embryonic development to adulthood (Cheah et al., 2012; Kalume et al., 2007; Kalume et al., 2013; Oakley et al., 2009; Yu et al., 2006). First, the *Scn1a*$^{+/-}$ mutations affects early development as indicated by small number of litters that survive until weaning (PND21), a lethality that is independent of seizures. We found that *Abhd6*$^{+/-}$ and *Abhd6*$^{-/-}$ mutations do not influence this phenotype as indicated by no obvious change in number of surviving litters and number of pups per litter measured at PND21 when crossed with *Scn1a*$^{+/-}$. This result shows that there are no signicant genetic interactions between *Scn1a*$^{+/-}$, *Abhd6*$^{+/-}$ and *Abhd6*$^{-/-}$ mutations during early development. The later period between PND21–45 is characterized by increased seizure-dependent lethality and SUDEP. We show that *Abhd6*$^{+/-}$ mutation rescues *Scn1a*$^{+/-}$ pup lethality during this period, suggesting that ABHD6 might represent a tractable enzyme for development of targeted therapeutics to protect against seizures in *Scn1a*$^{+/-}$ mice. Accordingly, *Abhd6*$^{+/-}$ and *Abhd6*$^{-/-}$ mutations and ABHD6 inhibition reduce thermal seizure duration in *Scn1a*$^{+/-}$ pups during PND21–35. Furthermore, ABHD6 inhibition reduces thermal seizure incidence measured in *Scn1a*$^{+/-}$ pups during PND21–35 using a low-fever paradigm. However, the conversion of a protective effect in heterozygous null *Abhd6* mice to a susceptibility effect in homozygous *Abhd6* mice reduces enthusiasm to some extent for targeting *Abhd6* for therapeutic purposes as this points to potentially harmful effects of targeting this gene, and shows that further optimization of this therapeutic approach is needed, including optimization of compound that might only partially and transiently inhibit ABHD6 activity, for example competitive inhibitors compared to irreversible inhibitors such as KT-182. Furthermore, it remains important to determine how *Abhd6* expression and activity compare through development in in wild type and *Scn1a*+/− mice and in patient diagnosed with DS? Such information may have implications for understanding the lack of an effect of the Abhd6$^{-/-}$ allele on survival and the potential value of long-term targeting of Abhd6 in DS particularly in older children and adults.

The third period of increased lethality occurs follows PND45 and does not involve seizures. We found that *Abhd6*$^{+/-}$ mutation does not influence this phenotype. By sharp contrast, we show that *Abhd6*$^{-/-}$ mutation increases *Scn1a*$^{+/-}$ pup lethality between PND21–35, despite reducing the duration of thermally induced seizure to the same extent as *Abhd6*$^{+/-}$ mutation and ABHD6 inhibition. These results suggest that absence of ABHD6 expression might accelerate *Scn1a*$^{+/-}$-mediated disease progression through a different mechanism than control of seizures. ABHD6 is a multifunctional protein that contains serine-dependent catalytic domain involved in 2-AG hydrolysis and a protein-interacting domain involved in the trafficking of AMPA receptor subunits to the plasma membrane (Bakas et al., 2017). Accordingly, genetic deletion of ABHD6 expression will likely impair AMPA receptors during early development, which is likely to enhance the detrimental effect of *Scn1a*$^{+/-}$ on early development. Thus, our study shows that *Abhd6*$^{+/-}$ and *Abhd6*$^{-/-}$ mutations differently influence disease progression resulting from *Scn1a*$^{+/-}$, a result that emphasizez the need to further optimize this therapeutic approach.

3.3. ABHD6 inhibition, seizures and preclinical relevance

ABHD6 inhibition reduces the duration of seizures without affecting either the temperature required to trigger them or their severity. Reduced threshold to thermal seizures is the most common effect of $GABA_AR$-deficits in mouse models of developmental epilepsies as demonstrated with γ2 subunit mutations in synaptic $GABA_AR$ (Hill et al., 2011; Martin et al., 2010). Considering that: 1) the binding site of picrotoxin is on the β3 subunit of $GABA_AR$ (Chen et al., 2006), and 2) 2-AG binds to the β2 subunit of the $GABA_AR$ and modulates δ subunit containing extrasynaptic $GABA_AR$, our data suggest that increased 2-AG levels resulting from KT-182 treatment and its allosteric potentiation of extrasynaptic $GABA_AR$ function should not influence the temperature as the antagonists picrotoxin does (Supplementary Fig. S3). Thus, differences in the binding of sites of 2-AG and picrotoxin on $GABA_AR$ subunits (β2 versus β3) may differentially modulate these receptors and their physiological results; similar to BZs that act on α1β2γ2-$GABA_ARs$ through key residues within the N-terminal region of α subunits to render their sedative and anxiolytic actions (Walters et al., 2000). Furthermore, this differential in vivo response of picrotoxin and KT-182 on threshold seizure agrees with its proposed mechanism of action that involves potentiation of tonic $GABA_AR$ currents in dentate GCs identified by electrophysiological recording of dentate GCs, which reduce hyperexcitation frequency and do not affect its amplitude (Mitchell and Silver, 2003).

Given the anti-seizure characteristics of ABHD6 inhibition (reduction in seizure incidence and duration and no effect on severity), its MOA (potentiation of tonic $GABA_AR$ currents through a BDZ-independent mechanism) and its promising safety profile, our results suggest that ABHD6-inhibition represents a promising candiate for combination therapeutic approaches to improve the control of seizures. An exciting outcome would be to develop a combination therapy that reduces the doses of BDZ required to reduce seizures when adding an ABHD6 inhibitor, thereby achieving seizure control and reducing the known side effects linked to BDZ treatment (Barker et al., 2004; Chamberlain et al., 2014; Devinsky et al., 2018). Remarkably, we found increased tonic $GABA_AR$ current capacity in dentate GCs of surviving *Scn1a*$^{+/-}$ pups. Since surviving *Scn1a*$^{+/-}$ pups exhibit lower baseline GABAergic interneuron excitability (Yu et al., 2006) and increased extrasynaptic $GABA_AR$ function (our data), it is likely that direct targeting of these receptors, for example with agonists at $GABA_AR$ d-subunits, might show enhanced anti-seizure efficacy in *Scn1a*$^{+/-}$ mice and possibly in DS patients (Chuang and Reddy, 2018; Farrant and Nusser, 2005). Thus, the anti-seizure response linked to ABHD6 inhibition involves a distinct MOA than currently available AEM, which control both seizure duration and severity, and does not appear to be associated with tolerance or overt side-effects (Deng et al., 2021; Naydenov et al., 2014; Oakley et al., 2013). The increased survival and decreased sensitivity to hyperthermia-induced seizure observed in *Scn1a*$^{+/-}$,*Abhd6*+/− pups compared to *Scn1a*$^{+/-}$ pups highlights the significance of the interaction between these genes highlights several important next steps: includig how does pharmacological inhibition of ABHD6 or its heterozygous genetic deletion affect spontaneous seizure frequency or severity in DS animals as measured by long-duration EEG monitoring. This first outstanding question will require optimization daily treatment regimens and possibly selection of the pharmacological agent. The second outstanding question is whether early chronic inhibition of Abhd6 and acute inhibition

of Abhd6 later in life will influence cognitive and behavioral deficits in the model; as, unfortunately, no current DS treatments are available to help with such devastating cognitive and social impairments.

In conclusion, we report a molecular interaction that links ABHD6 activity to tonic $GABA_AR$ currents and controls hippocampal hyperexcitability, a mechanism that can be targeted to dampen seizures and reduce premature death in a preclinical mouse model of DS. In a paradigm that mimics low to moderate fever, ABHD6 inhibition increased the likelihood of being seizure free and reduced the duration of seizures, emphasizing the preclinical relevance of our results. Furthermore, tonic $GABA_AR$ currents in dentate GCs are significantly increased in *Scn1a*$^{+/-}$ pups (P35-P45, survivors), suggesting a compensatory mechanism to reduce seizure susceptibility in surviving *Scn1a*$^{+/-}$ mice that might favor the therapeutic efficacy of ABHD6 inhibitors. Thus, ABHD6 inhibitors represent a promising new therapeutic approach for the safe treatment of seizures in DS.

4. Material and methods

4.1. Animals

Scn1a$^{+/-}$ and *Abhd6*$^{-/-}$ mice (Van Esbroeck et al., 2019; Yu et al., 2006) and their heterozygous progeny were crossed >20 generations to C57BL/6 mice to generate the mice used in this study. All animal care and use conformed to the National Institutes of Health Guide for Care and Use of Laboratory Mice and was approved by the University of Washington Institutional Animal Care and Use Committee.

4.2. Drugs

KT-182 (2 mg/kg, IP), a generous gift from Dr. Ku-Lung Hsu (University of Virginia) or vehicle (1:1:18 cremaphore: ethanol:PBS) was given 3 h prior to behavioral experiments. Picrotoxin (1 mg/kg, Tocris, # 1128 diluted in 3% DMSO: 97% saline) was given IP at a sub-seizure dose of 1 mg/kg 10 min prior to behavioral experiments. Specifics about GABA and GABAzine are in (Kaplan et al., 2013).

4.3. Thermal inductions

Mice of both sexes (P22–34) were group housed and maintained on a standard 12-h light-dark cycle. Following treatment with drug(s) or vehicle, each animal was placed in a plexi-glass chamber and each animal's core body temperature (**T**°) was continuously monitored by a rectal T° probe and controlled by a feedback circuit in line with a heat lamp. Mice were allowed to acclimate in the chamber for 10 min and then their body T° was increased in 0.5 °C steps at 2-min intervals until a seizure occurred or a T° of 41 °C was reached (Figs. 2A). The animal was then cooled and returned to its home-cage. The induction process and resulting seizures were recorded by video monitoring and reviewed to determine the duration of the seizure, the T° at which the seizure occurred and the severity of the seizure using the Racine scale system (1, mouth and facial movements; 2, head nodding; 3, forelimb clonus, usually one limb; 4, forelimb clonus with rearing; and 5, generalized tonic-clonic seizure, rearing, clonus, and falling over) (Racine, 1972). A second prolonged, thermal induction paradigm that mimics a low fever was used on separate

animals (Fig. 2G). Following injection of drug or vehicle the animals were placed in the recording chamber, acclimated for 10 min and their body T° was raised 0.5 °C everyone 2 min up to 38 °C and held at this T° for 30 min. The number of seizures during the 30 min, the seizure severity and duration were evaluated and compared between drug-treated and vehicle-treated animals.

4.4. Brain slices and electrophysiology

Fresh brain slices were prepared acutely for each experiment, and electrophysiology recording was performed as described (Kaplan et al., 2013). Briefly, mice of both sexes were group housed and maintained on a 12 h "light-dark" cycle. Mice (P25–45) were anesthetized with iso-flurane and then decapitated. Whole brains were isolated and immersed in a chilled sucrose-based cutting solution containing the following (in mM): 87 NaCl, 1.25 NaH_2PO_4, 2.5 KCL, 7 $MgCl_2$, 25 $NaHCO_3$, 0.5 $CaCl_2$, 25 D-glucose, 75 sucrose, and bubbled with 95% O_2/5% CO_2, pH 7.4. Transverse slices (400 μM) were made with a vibrating tissue slicer (Vibratome). Slices were incubated for one hour in warmed artificial cerebral spinal fluid (**aCSF;** 33 ± 1 °C) containing the following (in mM): 125 NaCl, 1.25 NaH_2PO_4, 26 $NaHCO_3$, 3 KCl, 10 D-glucose, 2 $MgCl_2$, 2 $CaCl_2$, and bubbled with 95% O_2/5% CO_2, pH 7.4. Kynurenic acid (1 mM) was included in the dissection, incubation, and holding solutions, but was omitted from the experimental solutions. After 1 h., slices were held in aCSF at 22–23 °C until used.

Transverse slices of unilateral hemispheres were placed in a submersion chamber on an upright microscope and viewed with an Olympus 40× (0.9 N.A.; BX51WI) water-immersion objective with differential interference contrast and infrared optics and were perfused with oxygenated aCSF at a rate of 2 mL/min. Dentate GCs were identified by their location, appearance, and physiological properties. Whole-cell recordings were made using patch pipettes constructed from thick-walled borosilicate glass capillaries and filled with intracellular solutions (resistances ranging between 2.5 and 5 MΩ) optimized for current-clamp recordings to measure action potentials, or voltage-clamp recordings to measure sIPSCs or sEPSCs, as described below. The intracellular solution for all current-clamp experiments was as follows (in mM): 132.3 K-gluconate, 7.7 KCl, 4 NaCl, 0.5 $CaCl_2$, 10 Hepes, 5 EGTA free acid, 4 ATP Mg^{2+} salt, 0.5 GTP Na^+ salt, pH buffered to 7.2–7.3 with KOH. The intracellular solution for measuring sIPSCs (V_h = −60 mV; E_{Cl} = 0 mV) in voltage clamp was as follows (in mM): 130 CsCl, 4 NaCl, 0.5 $CaCl_2$, 10 Hepes, 5 EGTA, 4 ATP Mg^{2+} salt, 0.5 GTP Na^+ salt, 5 QX-314, pH buffered to 7.2–7.3 with CsOH. Note that this results in $GABA_A$R-mediated currents to be inward (downward deflections in the displays of holding current). Therefore, enhancement of tonic GABAAR-mediated currents corresponds to sustained inward currents. sIPSCs were measured in the presence of ionotropic glutamate receptor antagonists, CNQX (20 μM) and APV (50 μM). The intracellular solution for measuring sEPSCs (V_h = −60 mV); E_{Cl} = −60 mV) in voltage clamp was as follows (in mM): 145 Cs-gluconate, 2 $MgCl_2$, 10 Hepes, 0.5 EGTA, 2 ATP-Tris, 0.2 GTP Na^+ salt, pH buffered to 7.2–7.3 with CsOH. Recordings were obtained through a Multiclamp 700A amplifier (Molecular Devices). Drugs were dissolved in aCSF and bath-applied for a minimum of 7 min before analysis. Data were analyzed using pClamp (version 6.3) software (Axon Instruments). For analysis of tonic currents, holding currents

prior and after drug were compared by fitting the Gaussian distribution of all data points not skewed by synaptic events from a point 3 pA to the left of the peak value to the rightmost (smallest) histogram distribution (histograms are shown in figures). Drug induced changes in tonic $GABA_AR$ current magnitude and sIPSC frequency was calculated by comparing the amplitude/frequency in the drug versus the mean amplitude/frequency of the currents before drug application. Only one recording was made per brain slice. Access resistance was continuously monitored for each cell. Cells were discarded if access resistance changed by >15%. Only one cell was recorded from each brain slice.

4.5. Statistics

For assessment for electrophysiological and behavioral experiments, all data are expressed as mean ± SEM. Single-sample *t*-tests and independent-sample *t*-tests were used where indicated. In the cases where ANOVA revealed significant main effects or interactions, we conducted post hoc comparisons using the Student-Newman-Keuls method. The Mantel-Cox test is used to compare the survival distributions of two samples. In all cases, statistical comparisons were two-tailed, and the significance threshold was set at $P < 0.05$. For figures, $^{\#}P < 0.1$; $^{*}P < 0.05$; $^{**}P < 0.01$; < 0.001.

Supplementary Material

Refer to Web version on PubMed Central for supplementary material.

Acknowledgments

Special thanks to Dr. William Catterall and Simar Singh (University of Washington, Seattle) for critical reading of the manuscript.

Funding

National Institutes of Health grant NS098777 (NS) and NS118130 (NS).

Data availability

Data will be made available on request.

Abbreviations:

2-AG	2-arachidonoyl glycerol
AEM	anti-epileptic drugs
AP	action potential
ABHD6	alpha/beta-hydrolase domain containing 6
aCSF	artificial cerebral spinal fluid
CB_1R	cannabinoid receptor 1
DG	dentate gyrus

DS	Dravet Syndrome
GABA	gamma-aminobutyric acid
$GABA_AR$	gamma-animobutyric acid receptors A
GC	granule cell
KO	knockout
MOA	mechanism of action
PTX	picrotoxin
PTZ	pentylenetetrazole
SUDEP	sudden unexpected death in epilepsy
WT	wildtype

References

Anderson LL, et al. , 2019. Coadministered cannabidiol and clobazam: preclinical evidence for both pharmacodynamic and pharmacokinetic interactions. Epilepsia. 60, 2224–2234. [PubMed: 31625159]

Bakas T, et al. , 2017. The direct actions of cannabidiol and 2-arachidonoyl glycerol at GABAA receptors. Pharmacol. Res 119, 358–370. [PubMed: 28249817]

Barker MJ, et al. , 2004. Persistence of cognitive effects after withdrawal from long-term benzodiazepine use: a meta-analysis. Arch. Clin. Neuropsychol 19, 437–454. [PubMed: 15033227]

Brickley SG, Mody I, 2012. Extrasynaptic GABAA receptors: their function in the CNS and implications for disease. Neuron. 73, 23–34. [PubMed: 22243744]

Cao JK, et al. , 2019. ABHD6: its place in endocannabinoid signaling and beyond. Trends Pharmacol. Sci 40 (4), 267–277. [PubMed: 30853109]

Catterall WA, 2017. Dravet syndrome: a sodium channel interneuronopathy. Curr. Opin. Physiol 42–50. [PubMed: 30123852]

Chamberlain JM, et al. , 2014. Lorazepam vs diazepam for pediatric status epilepticus: a randomized clinical trial. Jama. 311, 1652–1660. [PubMed: 24756515]

Cheah CS, et al. , 2012. Specific deletion of NaV1. 1 sodium channels in inhibitory interneurons causes seizures and premature death in a mouse model of Dravet syndrome. Proc. Natl. Acad. Sci 109, 14646–14651. [PubMed: 22908258]

Chen L, et al. , 2006. Structural model for γ-aminobutyric acid receptor noncompetitive antagonist binding: widely diverse structures fit the same site. Proc. Natl. Acad. Sci 103, 5185–5190. [PubMed: 16537435]

Chuang S-H, Reddy DS, 2018. Genetic and molecular regulation of extrasynaptic GABA-A receptors in the brain: therapeutic insights for epilepsy. J. Pharmacol. Exp. Ther 364, 180–197. [PubMed: 29142081]

Colasante G, et al. , 2020. dCas9-based Scn1a gene activation restores inhibitory interneuron excitability and attenuates seizures in Dravet syndrome mice. Mol. Ther 28, 235–253. [PubMed: 31607539]

Deng L, et al. , 2021. ABHD6 controls amphetamine-stimulated Hyperlocomotion: involvement of CB1 receptors. Cannabis Cannabinoid Res. 7 (2), 188–189. [PubMed: 34705543]

Dengler CG, Coulter D, 2016. Normal and epilepsy-associated pathologic function of the dentate gyrus. Prog. Brain Res 226, 155–178. [PubMed: 27323942]

Devinsky O, et al. , 2018. Effect of cannabidiol on drop seizures in the Lennox–Gastaut syndrome. N. Engl. J. Med 378, 1888–1897. [PubMed: 29768152]

Dravet C, 2011. The core Dravet syndrome phenotype. Epilepsia. 52, 3–9.

Farrant M, Nusser Z, 2005. Variations on an inhibitory theme: phasic and tonic activation of GABA a receptors. Nat. Rev. Neurosci 6, 215–229. [PubMed: 15738957]

Golovko T, et al. , 2014. Control of inhibition by the direct action of cannabinoids on GABAA receptors. Cereb. Cortex 25, 2440–2455. [PubMed: 24646614]

Griffin A, et al. , 2018. Preclinical animal models for Dravet syndrome: seizure phenotypes, comorbidities and drug screening. Front. Pharmacol 9, 573. [PubMed: 29915537]

Hill EL, et al. , 2011. Temperature elevation increases GABAA-mediated cortical inhibition in a mouse model of genetic epilepsy. Epilepsia. 52, 179–184. [PubMed: 21219304]

Hsu K-L, et al. , 2013. Discovery and optimization of piperidyl-1, 2, 3-triazole ureas as potent, selective, and in vivo-active inhibitors of α/β-hydrolase domain containing 6 (ABHD6). J. Med. Chem 56, 8270–8279. [PubMed: 24152295]

Ito S, et al. , 2013. Mouse with Nav1. 1 haploinsufficiency, a model for Dravet syndrome, exhibits lowered sociability and learning impairment. Neurobiol. Dis 49, 29–40. [PubMed: 22986304]

Kalume F, et al. , 2007. Reduced sodium current in Purkinje neurons from Nav1. 1 mutant mice: implications for ataxia in severe myoclonic epilepsy in infancy. J. Neurosci 27, 11065–11074. [PubMed: 17928448]

Kalume F, et al. , 2013. Sudden unexpected death in a mouse model of Dravet syndrome. J. Clin. Invest 123, 1798–1808. [PubMed: 23524966]

Kaplan JS, et al. , 2013. Opposite actions of alcohol on tonic GABA a receptor currents mediated by nNOS and PKC activity. Nat. Neurosci 16, 1783–1793. [PubMed: 24162656]

Korff C, et al. , 2007. Dravet syndrome (severe myoclonic epilepsy in infancy): a retrospective study of 16 patients. J. Child Neurol 22, 185–194. [PubMed: 17621480]

Krook-Magnuson E, et al. , 2015. In vivo evaluation of the dentate gate theory in epilepsy. J. Physiol 593, 2379–2388. [PubMed: 25752305]

Liautard C, et al. , 2013. Hippocampal hyperexcitability and specific epileptiform activity in a mouse model of D ravet syndrome. Epilepsia. 54, 1251–1261. [PubMed: 23663038]

Manterola A, et al. , 2018. Deregulation of the endocannabinoid system and therapeutic potential of ABHD6 blockade in the cuprizone model of demyelination. Biochem. Pharmacol Nov 157, 189–201. [PubMed: 30075103]

Martin MS, et al. , 2010. Altered function of the SCN1A voltage-gated sodium channel leads to γ-aminobutyric acid-ergic (GABAergic) interneuron abnormalities. J. Biol. Chem 285, 9823–9834. [PubMed: 20100831]

McCartney MR, et al. , 2007. Tonically active GABAA receptors in hippocampal pyramidal neurons exhibit constitutive GABA-independent gating. Mol. Pharmacol 71, 539–548. [PubMed: 17090706]

Meera P, et al. , 2011. Molecular basis for the high THIP/gaboxadol sensitivity of extrasynaptic GABAA receptors. J. Neurophysiol 106, 2057–2064. [PubMed: 21795619]

Mitchell SJ, Silver RA, 2003. Shunting inhibition modulates neuronal gain during synaptic excitation. Neuron. 38, 433–445. [PubMed: 12741990]

Naydenov AV, et al. , 2014. ABHD6 blockade exerts antiepileptic activity in PTZ-induced seizures and in spontaneous seizures in R6/2 mice. Neuron. 83, 361–371. [PubMed: 25033180]

Oakley JC, et al. , 2009. Temperature-and age-dependent seizures in a mouse model of severe myoclonic epilepsy in infancy. Proc. Natl. Acad. Sci 106, 3994–3999. [PubMed: 19234123]

Oakley JC, et al. , 2013. Synergistic GABA-enhancing therapy against seizures in a mouse model of Dravet syndrome. J. Pharmacol. Exp. Ther 345, 215–224. [PubMed: 23424217]

Ogiwara I, et al. , 2007. Nav1. 1 localizes to axons of parvalbumin-positive inhibitory interneurons: a circuit basis for epileptic seizures in mice carrying an Scn1a gene mutation. J. Neurosci 27, 5903–5914. [PubMed: 17537961]

Racine RJ, 1972. Modification of seizure activity by electrical stimulation: II. Motor seizure. Electroencephalogr. Clin. Neurophysiol 32, 281–294. [PubMed: 4110397]

Rudolph U, Knoflach F, 2011. Beyond classical benzodiazepines: novel therapeutic potential of GABA a receptor subtypes. Nat. Rev. Drug Discov 10, 685. [PubMed: 21799515]

Schipper S, et al. , 2016. Tonic GABA a receptors as potential target for the treatment of temporal lobe epilepsy. Mol. Neurobiol 53, 5252–5265. [PubMed: 26409480]

Sigel E, et al. , 2011. The major central endocannabinoid directly acts at GABA(a) receptors. Proc. Natl. Acad. Sci. U. S. A 108, 18150–18155. [PubMed: 22025726]

Tchantchou F, Zhang Y, 2013. Selective inhibition of alpha/beta-hydrolase domain 6 attenuates neurodegeneration, alleviates blood brain barrier breakdown, and improves functional recovery in a mouse model of traumatic brain injury. J. Neurotrauma 30, 565–579. [PubMed: 23151067]

Van Esbroeck ACM, et al. , 2019. Identification of α, β-hydrolase domain containing protein 6 as a diacylglycerol lipase in neuro-2a cells. Front. Mol. Neurosci 12, 286. [PubMed: 31849602]

Walters RJ, et al. , 2000. Benzodiazepines act on GABAA receptors via two distinct and separable mechanisms. Nat. Neurosci 3, 1274–1281. [PubMed: 11100148]

Wen J, et al. , 2015. Activation of CB2 receptor is required for the therapeutic effect of ABHD6 inhibition in experimental autoimmune encephalomyelitis. Neuropharmacology. 99, 196–209. [PubMed: 26189763]

Wlodarczyk AI, et al. , 2013. GABA-independent GABAA receptor openings maintain tonic currents. J. Neurosci 33, 3905–3914. [PubMed: 23447601]

Xu X, et al. , 2014. Early clinical features and diagnosis of Dravet syndrome in 138 Chinese patients with SCN1A mutations. Brain and Development 36, 676–681. [PubMed: 24168886]

Yu FH, et al. , 2006. Reduced sodium current in GABAergic interneurons in a mouse model of severe myoclonic epilepsy in infancy. Nat. Neurosci 9, 1142. [PubMed: 16921370]

Zareie P, et al. , 2018. Anticonvulsive effects of endocannabinoids; an investigation to determine the role of regulatory components of endocannabinoid metabolism in the Pentylenetetrazol induced tonic-clonic seizures. Metab. Brain Dis 33, 939–948. [PubMed: 29504066]

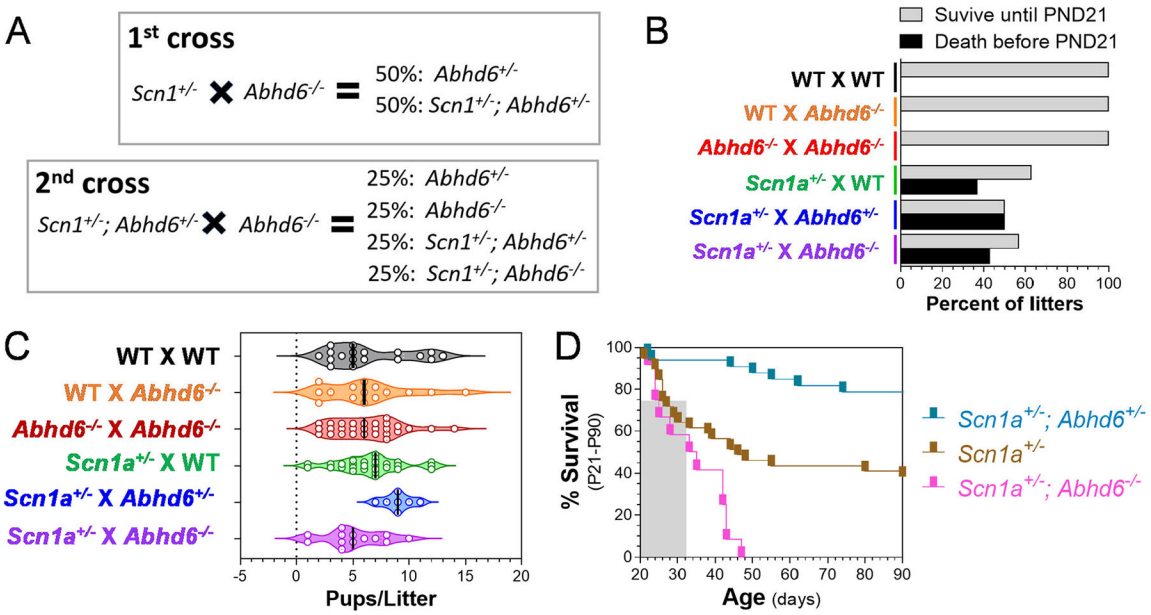

Fig. 1.

Abhd6$^{+/-}$ reduces and *Abhd6*$^{-/-}$ worsens premature lethality of *Scn1a*$^{+/-}$ pups. A] Breeding strategy to generate *Scn1a*$^{+/-}$; *Abhd6*$^{+/-}$ pups, *Scn1a*$^{+/-}$; *Abhd6*$^{+/-}$ pups, and littermate controls. B] Survival and premature death of pups (PND0–21) in litters delivered by each genetic cross (Surviving litters had at least 1 pup at weaning). Results show $n = 14–24$ independent litters for each cross. C. Litter size (i.e., number of pups per litters at weaning, PND21). Results show 2–15 pups/litters for each cross (Total: $n = 109$ litters). Analysis by Ordinary One-Way ANOVA followed by Dunnett's multicomparaison test shows no significant difference from WT X WT cross (> 0.05). D] *Scn1a*$^{+/-}$; *Abhd6*$^{+/-}$ pups (acqua) lived significantly longer than *Scn1a*$^{+/-}$ pups (brown), whereas *Scn1a*$^{+/-}$; *Abhd6*$^{-/-}$ pups (pink) lived significantly shorter. Mantel-Cox test: $P < 0.001$. $N = 39$ *Scn1a*$^{+/-}$ pups, 32 *Scn1a*$^{+/-}$; *Abhd6*$^{+/-}$ pups and 12 *Scn1a*$^{+/-}$; *Abhd6*$^{-/-}$ pups.

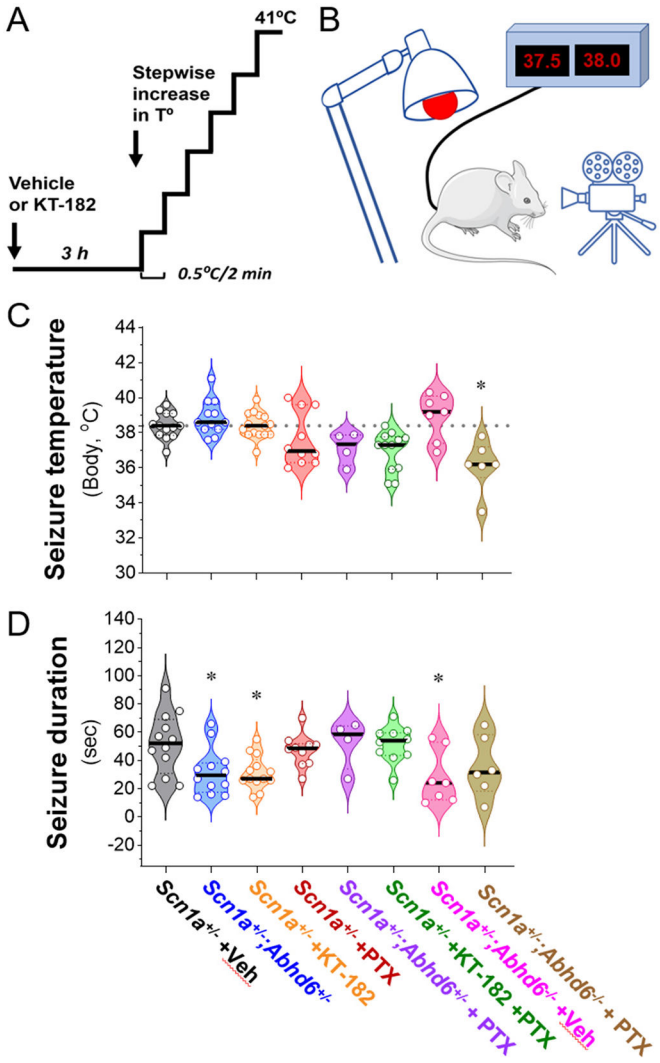

Fig. 2.

Blocking ABHD6 activity reduced the duration of thermally induced seizures in *Scn1a*$^{+/-}$ pups. A] Schematic of the thermal induction of seizures protocol. *Scn1a*$^{+/-}$ pups (PND21–35) were injected with either vehicle (1:1:18, cremophore, ethanol, buffer), the ABHD6 inhibitor KT-182 (2 mg/kg, i.p.) (3 h pretreatment) and/or a subthreshold doses of the $GABA_AR$ antagonist picrotoxin (PTX, 1 mg/kg). Their body temperature was recorded and increased by 0.05 °C every 2 min until either a seizure occurs, or the body temperature reached 41 °C. B] Body temperature was increased using a heat lamp and behavioral seizures were videorecorded and analyzed offline. C] *Abhd6*$^{+/-}$ and *Abhd6*$^{-/-}$ mutations, as well as pretreatment with KT-182, PTX, and KT-182 + PTX, did not affect the average temperature that triggers thermally induced seizures of *Scn1a*$^{+/-}$ pups compared to vehicle treated *Scn1a*$^{+/-}$ pups. Pretreatment of *Scn1a*$^{+/-}$; *Abhd6*$^{-/-}$ pups with PTX reduced the average temperature that triggers thermally induced seizures. Results are mean ± S.E.M. from 4 to 15 pups. Ordinary One-Way ANOVA followed by Dunnett's multicomparaison test. *$P < 0.05$. D] *Abhd6*$^{+/-}$ and *Abhd6*$^{-/-}$ mutations, as well as pretreatment with KT-182

reduced seizure duration [*sec*] in *Scn1a*$^{+/-}$ pups. Results are mean ± S.E.M. from 4 to 15 pups. Ordinary One-Way ANOVA followed by Dunnett's multicomparaison test. *$P < 0.05$.

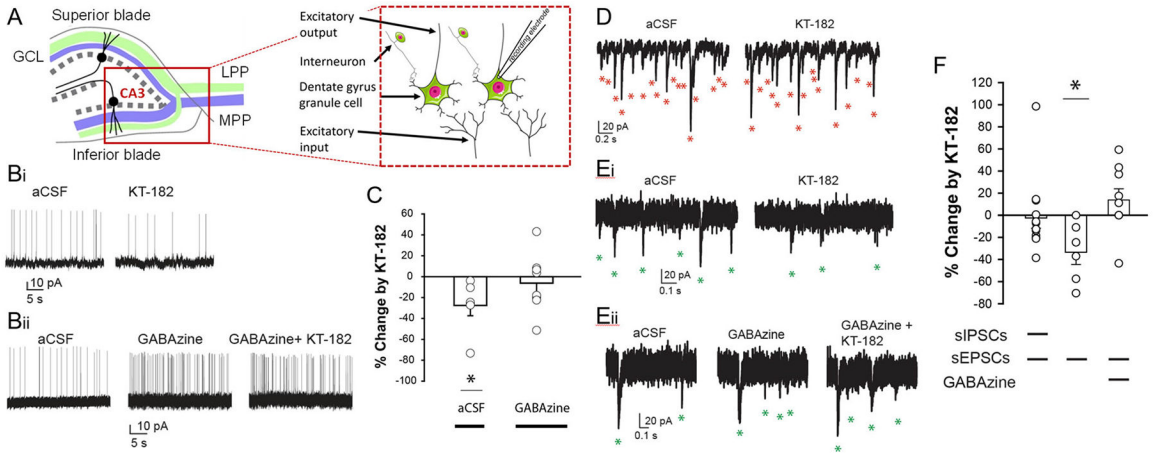

Fig. 3.

KT-182 reduces the excitatory output from the dentate gyrus measured in hippocampal slices from *Scn1a*$^{+/-}$ pups. Effect of the ABHD6 inhibitor, KT-182, on action potential, sIPSCs and sEPSCs in hippocampal slices from *Scn1a*$^{+/-}$ pups (PND35–45) as measured by current-clamp recordings and treatment with GABAzine, a antagonist of phasic (synaptic) $GABA_A$Rs. A] Diagram depicting the CA3 region of the hippocampus and a closer view of the dentate gyrus granule cells (GC) that were recorded using slice electrophysiology. B] Representative current-clamp recordings of action potentials (AP) measured in GCs from a *a*$^{+/-}$ hippocampal slices: in aCSF (basal control, left) and KT-182 (100 nM; right) (Bi), and in aCSF (basal control, left), GABAzine (10 μM; middle) and GABAzine + KT-182 (100 nM; right) (Bii). Each upward deflection represents the membrane depolarization and repolarization from a single AP. C] Mean % changes in AP frequency caused by GABAzine (10 μM), KT-182 (100 nM), and KT-182 + GABAzine. KT-182 reduced the AP frequency, while GABAzine alone increased the frequency. Data are mean ± S.E.M.; **P* < 0.05 vs. CTR (aCSF) when using dependent variable presented is % change, these are one-sample *t*-tests. D] Representative voltage-clamp recordings of sIPSCs measured in GCs from a *Scn1a*$^{+/-}$ hippocampal slice (E_{Cl-} = 0 mV; V_h = −60 mV, CNQX, 20 mM and APV, 50 mM) in: aCSF (basal control, left) and KT-182 (100 nM, right). Red asterisks indicate each sIPSC. E] Representative voltage-clamp recordings of sEPSCs measured in GCs from a *Scn1a*$^{+/-}$ hippocampal slices (E_{Cl-} = −60 mV; V_h = −60 mV) in: aCSF (basal control, left) and KT-182 (100 nM, right) (Ei) and in aCSF (basal control, left), GABAzine (10 μM, middle), and GABAzine + KT-182 (right). Green asterisks indicate each sIPSC. F] Mean % changes in sIPSCs (*n* = 13) and sEPSCs caused by GABAzine (10 μM), KT-182 (100 nM), and KT-182 + GABAzine. Data are mean ± S.E.M. **P* < 0.05 when using Ordinary One-Way ANOVA followed by Dunnett's multicomparaison test. Specifics abjout data statistical analyses in B, D and E are in supplementary Table S2.

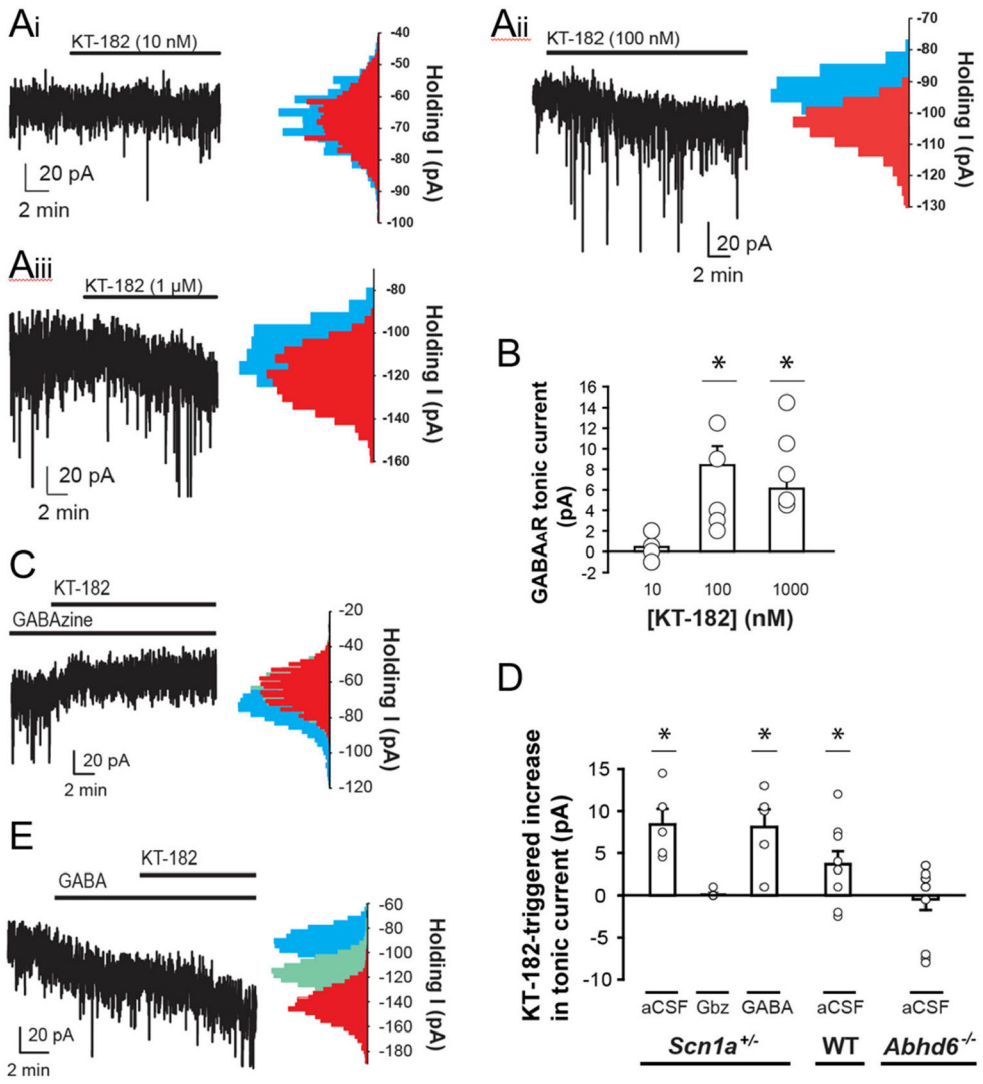

Fig. 4.

KT-182 enhances tonic $GABA_AR$-mediated inhibition in dentate gyrus granual cells measured in hippocampal slices from *Scn1a*$^{+/-}$ pups. Effect of the ABHD6 inhibitor, KT-182, on tonic $GABA_AR$-mediated currents in hippocampal slices of WT and *Scn1a*$^{+/-}$ pups (PND35–45) using whole cell patch recording, and treating with GABA and GABAzine, modulators of $GABA_AR$. A] Representative voltage-clamp recordings (E_{Cl-} = 0 mV; V_h = −60 mV) from dentate GCs (left) and average holding currents (right) in: aCSF (i.e., basal control; blue) and when pretreatet (6 min) with KT-182 (red) at either 10 nM (Ai), 100 nM (Aii), or 1 µM (Aiii). Red asterisks indicate each sIPSC. B] Summary of the KT-182-triggered increase in mean $GABA_AR$ currents. Data are mean ± S. E.M. *P < 0.05 vs. CTR (aCSF) when using one-tailed t-tests showing that both 100 nM and 1000 nM KT-182 caused changes in the tonic current. A one-way ANOVA that KT-182 (100 nM and 1 mM) increased the tonic current compared to KT-182 (10 nM), F (2,13) = 7.72, *P* < 0.01. C] Representative voltage-clamp recordings (E_{Cl-} = 0 mV; V_h = −60 mV) from dentate GCs (left) and average holding currents (right) in: aCSF (i. e., baseline control; blue) and

GABAzine (10 mM, green, i.e., behind blue), and in KT-182 (100 nM; red). D] Summary of the mean KT-182-triggered increase in $GABA_AR$ tonic currents. Data are mean ± S.E.M. *$P < 0.05$ when using one-way ANOVA. Specifics about data statistical analyses in B and E are in supplementary Table S2. E] Representative voltage-clamp recordings ($E_{Cl-} = 0$ mV; $V_h = -60$ mV) from dentate GCs (left) and average holding currents (right) in: aCSF (i. e., baseline control; blue), in GABA (200 nM; green) (C), and in KT-182 (100 nM; red).

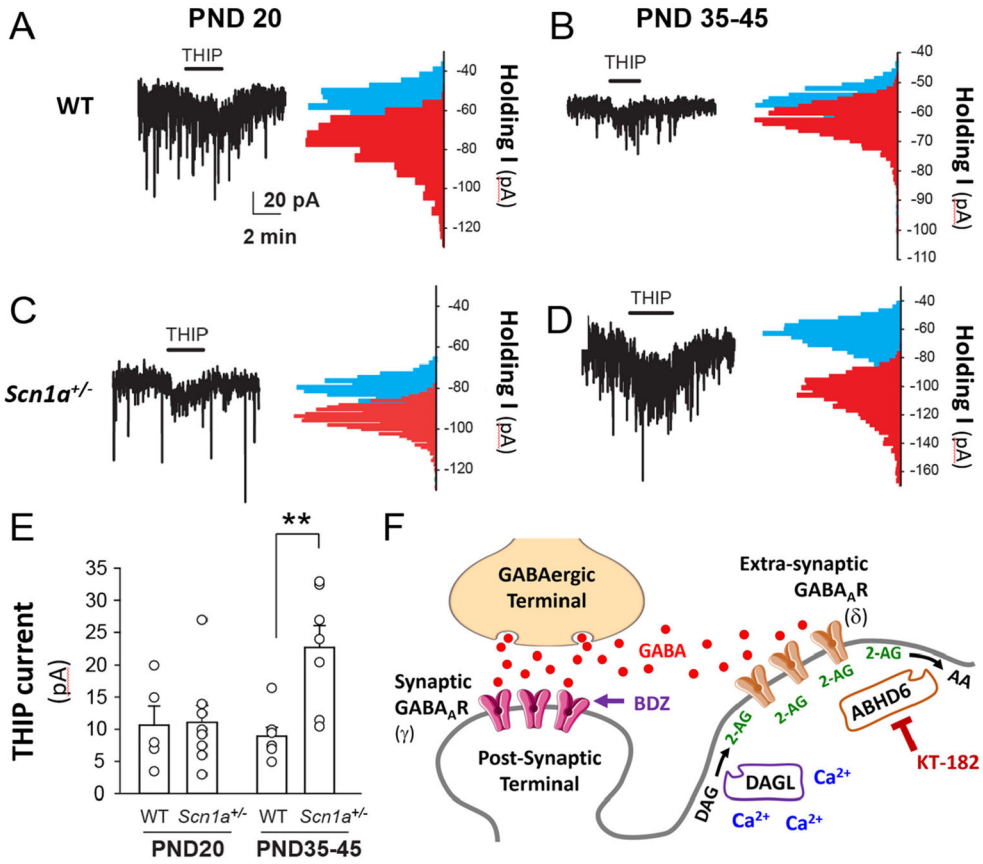

Fig. 5.

Scn1a$^{+/-}$ pups develop larger tonic $GABA_A$R-mediated currents in dentate gyrus granual cells measured in hippocampal slices at PND35–45 compared to PND20. Tonic $GABA_A$R-mediated currents in hippocampal slices from WT and *Scn1a*$^{+/-}$ pups at P20 and PND35–45 measured by whole cell patch recording and perfusing THIP. A-D] Representative voltage-clamp recordings from dentate GCs (E_{Cl-} = 0 mV; V_h = −60 mV) (left) and average holding currents (right) in: aCSF (baseline control, blue) followed by THIP treatment (500 nM) in: WT pups (PND20) (A), WT pups (P34–45) (B), *Scn1a*$^{+/-}$ pups (P20) (C), and *Scn1a*$^{+/-}$ pups (P34–45) (D). E] Summary of the mean THIP-induced currents between WT and *Scn1a*$^{+/-}$ pups at P20 and P34–45. Data are mean ± S.E.M. $P < 0.05$. *P < 0.05 when using two-way ANOVA showed a significant interaction between age and genotype, F (1,23) = 5.80, $P = 0.024$. Post hocs revealed that the THIP currents differed between WT and DS mice at PND 35–45. Specifics abjout data statistical analyses in B and E are in supplementary Table S2. F] Diagram of molecular interaction between ABHD6 and extrasynaptic $GABA_A$R. GABA is released from terimals and activates both synaptic $GABA_A$R (g-containing) and extrasynaptic $GABA_A$R (d-containing). Increase in intracellular calcium (Ca^{2+}) activated diacylglycerol lipase (DAGL), which hydrolyses diaglycerol (DAG) and releases 2-AG and fatty acids (not shown). KT-182 inhibition of ABHD6 and 2-AG accumulation represents the likely mediators that potentiates extrasynaptic $GABA_A$R. Amplitude and decay were also measured in Scn1+/− mice. Neither IPSC characteristic was affected by KT-182 (all $P >$

0.05). KT-182 had no effect on sIPSC amplitude (−6.36 +/− 3.17%, $n = 11$) nor decay time (−2.17 +/− 5.02%, n = 11).